

Supplementary Material:

Active Site Engineering of Intermetallic Nanoparticles by the Vapour-Solid Synthesis: Carbon Black Supported Nickel Tellurides for Hydrogen Evolution

Daniel Garstenaue^{a,b}, Patrick Guggenberger^{a,b}, Ondřej Zobač^c, Franz Jirsa^{d,e}, Klaus W. Richter^{a,f*}

^a Department of Functional Materials & Catalysis, University of Vienna, Josef-Holaubek-Platz 2, 1090 Vienna, Austria

^b Vienna Doctoral School in Chemistry, University of Vienna, Währinger Straße 42, 1090 Vienna, Austria

^c Institute of Physics of Materials, Czech Academy of Sciences, Žitkova 22, 61600 Brno, Czech Republic

^d Department of Inorganic Chemistry, University of Vienna, Josef-Holaubek-Platz 2, 1090 Vienna, Austria

^e Department of Zoology, University of Johannesburg, Auckland Park, 2006 Johannesburg, South Africa

^f X-ray Structure Analysis Centre, University of Vienna, Währinger Straße 42, 1090 Vienna, Austria

*Email: klaus.richter@univie.ac.at

Total X-Ray fluorescence spectroscopy

Recovery rate experiment tellurium

A recovery rate experiment was carried out to assure the accuracy of tellurium concentrations from TXRF investigations. Therefore, 500 μL of a $\beta_{\text{standard}}(\text{Te}) = 10 \text{ mg L}^{-1}$ tellurium standard solution, 500 μL of a 30 mg L^{-1} gallium standard solution, as internal standard, and 100 μL polyvinyl alcohol solution were mixed. 5 μL of the as-prepared mixture were drop cast onto the sample carrier and dried under IR irradiation for 45 min. After investigation by TXRF the correction factor for tellurium was calculated as $\beta_{\text{standard}}(\text{Te})$ over $\beta_{\text{TXRF}}(\text{Te})$. The observed factor was used to correct the tellurium concentrations of all investigated Ni-Te samples.

Table S 1.: TXRF tellurium recovery rate experiment

measurement	$\beta_{\text{TXRF}}(\text{Te}) [\text{mg L}^{-1}]$	correction factor
1	23.07	0.43
2	23.87	0.42
3	23.87	0.42
4	20.36	0.49
5	20.22	0.49

Sample quantification

Table S 2.: TXRF sample investigations (Te values are not corrected), 30 mg L⁻¹ gallium as internal standard

sample	weighed mass [mg]	$\beta(\text{Te})$ [mg L ⁻¹]	$\beta(\text{Ni})$ [mg L ⁻¹]
Ni/C_16	26.51	-	42.82
Ni ₈₅ Te ₁₅ /C	20.39	24.61	35.88
Ni ₇₈ Te ₂₂ /C	29.10	10.12	12.08
Ni ₄₉ Te ₅₁ /C	16.06	46.03	12.54
Ni ₃₉ Te ₆₁ /C	19.76	78.74	12.14
Ni/C_7	22.86	-	16.39
Ni ₆₇ Te ₃₃ /C	21.46	40.32	20.59
Ni ₈₅ Te ₁₅ /C	23.39	49.56	20.14

Powder X-Ray diffraction

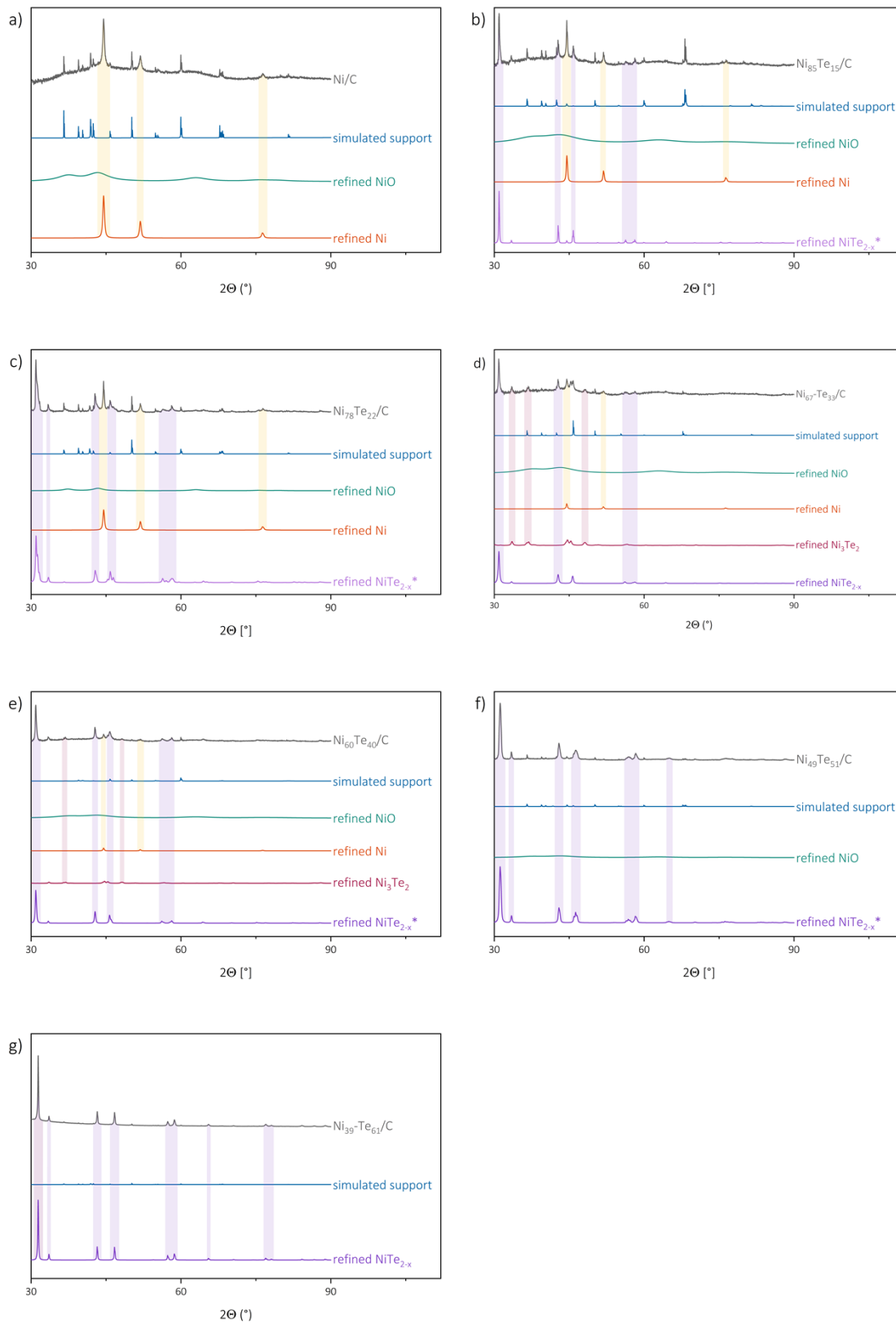


Figure S 1.: measured and refined tXRF patterns with the most significant peaks highlighted of Ni/C and intermetallic Ni-Te/C samples with ascending Te content from (a) to (g). *combined NiTe_{2-x} patterns with different parameter sets.

Physisorption

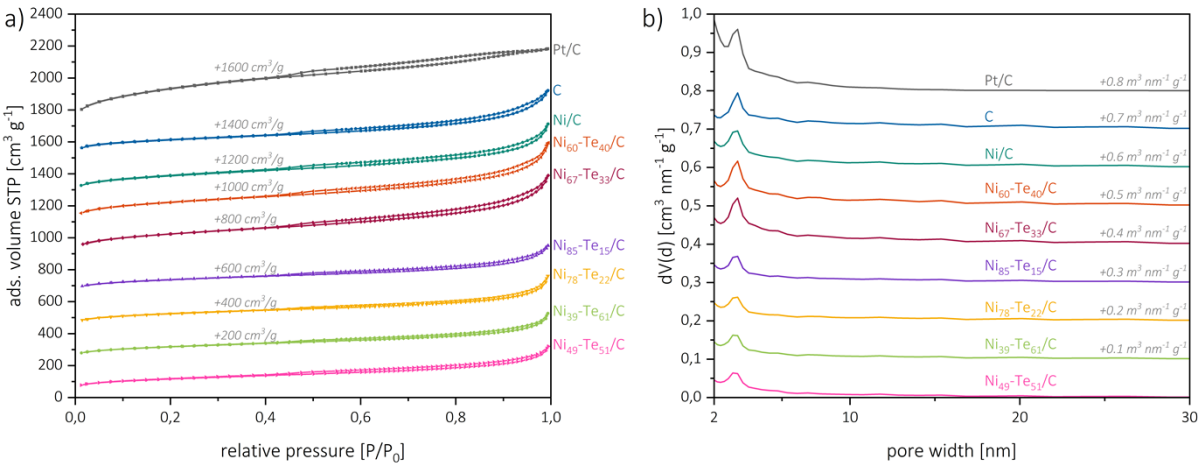


Figure S 2: Nitrogen physisorption isotherms recorded at $-196\text{ }^{\circ}\text{C}$ of carbon black based materials (a) and respective QSDFT pore size distributions (b).

Cyclic voltammetry

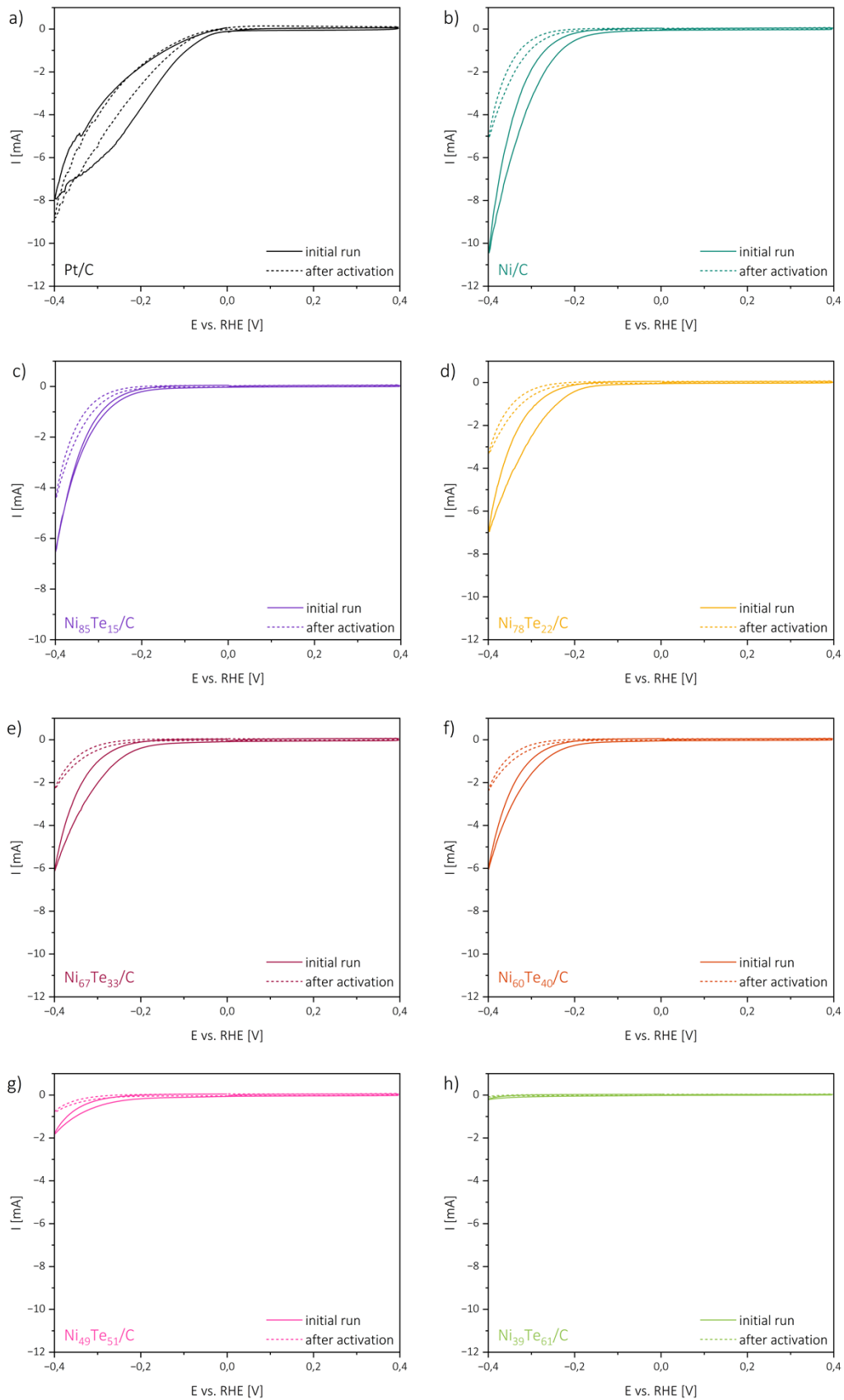


Figure S 3.: Cyclic voltammetry curves before and after activation from Pt/C (a); Ni/C (b); and intermetallic Ni-Te/C samples with ascending tellurium contents (d) to (h).

Double layer capacitance

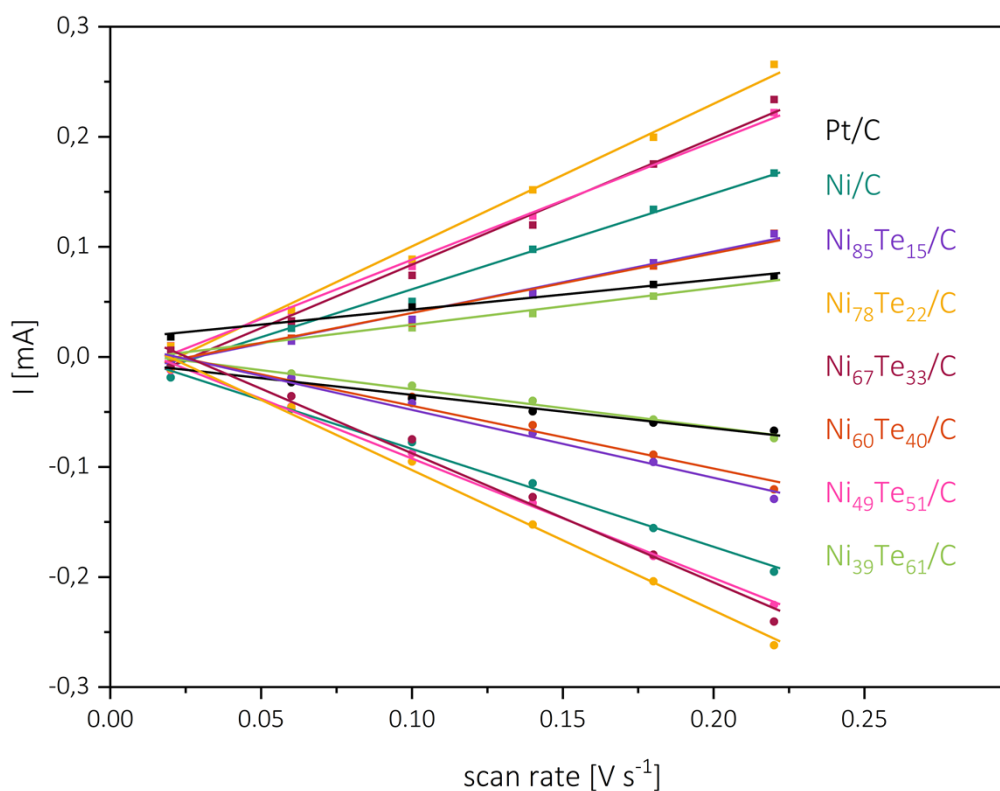


Figure S 4.: Cathodic (circles) and anodic (squares) charging currents measured at 0.10 V vs. RHE plotted as function of the scan rate. The determined double-layer capacitance of the system is taken as the average of the absolute value of the slope of the linear fits to the data.

Table S 3.: Calculated double layer capacitance (C_{DL}) of the prepared electrodes.

sample	C_{DL} [mF]
Pt/C	0.288
Ni/C	0.880
Ni ₈₅ Te ₁₅ /C	0.588
Ni ₇₈ Te ₂₂ /C	1.290
Ni ₆₇ Te ₃₃ /C	1.160
Ni ₆₀ Te ₄₀ /C	0.556
Ni ₄₉ Te ₅₁ /C	1.085
Ni ₃₉ Te ₆₁ /C	0.339